Search for effective Lorentz violation and CPT violation in ZEUS data

arxiv:2212.12750

A M Cooper-Sarkar
Low x 2023

WHY?

- A variety of models suggest Lorentz/CPT violation regimes are *possible*, for example:

  - String theory
  - Modified electrodynamics
  - "Boost-violating" models
  - Noncommutative field theory
  - Loop quantum gravity

  V. A. Kostelecký, S. Samuel, PLB **207**, 169 (1989) V. A. Kostelecký, R. Potting, NPB **359**, 545 (1991)
  S. Carroll et al., PRD **41**, 1231 (1990)
  S. Coleman, S. Glashow, PRD, **59**, 116008 (1999)
  S. Carroll et al., PRL **87**, 141601 (2001)
  X. Calmet et al., EPJC **23**, 363 (2002)
  J. Alfaro et al., PRL **84**, 2318 (2000)

- Lorentz/CPT violation could explain existing mysteries, such as:

  - baryogenesis of the universe
  - neutrino oscillations
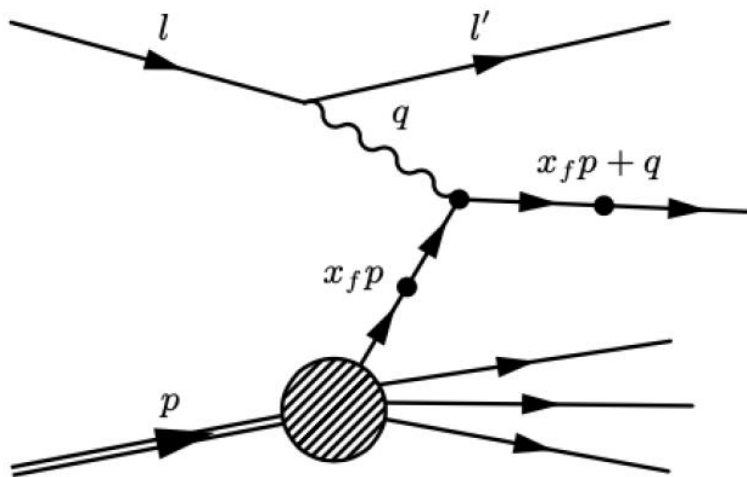 - the existence of photon and graviton

  O. Bertolami et al., PLB **395**, 178 (1997)
  V. A. Kostelecký, M. Mewes, PRD **70**, 031902 (2004)
  R. Bluhm and V.A. Kostelecký, PRD **71**, 065008 (2005)
  V. A Kostelecký, R. Potting, PRD **79**, 065018 (2009)

Some situations can be described in terms of an effective or apparent Lorentz violation (e.g. dark matter wind)

WHY at low x?

Extensions to the Standard Model (SME) with effective vector or tensor couplings produce effects at $x \sim 10^{-3}$

1

- Lorentz invariance = isotropy under rotations and relativistic boosts.
- Lorentz violation often implies CPT violation.
- Few studies of Lorentz/CPT violation in the quark sector
- Construct an Standard Model Extension with Lorentz Violation using 4D and 5D operators in context of Effective Field Theory

Interactions that we consider are ($q = u, d, s$):

$$\mathscr{L}_{SM} \ni \frac{1}{2} \bar{q} \gamma^\mu iD_\mu q + \mathrm{h.c.}$$

$$\mathscr{L}_{SME} \ni \frac{1}{2} c_q^{\mu\nu} \bar{q} \gamma_\mu iD_\nu q$$

$$- \frac{1}{2} a_q^{(5)\mu\alpha\beta} \bar{q} \gamma_\mu iD_{(\alpha} iD_{\beta)} q + \mathrm{h.c.}$$

This affects propagators and coupling

Not invariant under rotation of the particle fields

The 4-D c operators are CPT even and $\quad d\sigma \propto (f_f + f_{\bar{f}})$

**The 5-D a** operators are CPT odd and $\quad d\sigma \propto (f_f - f_{\bar{f}})$.

2

We are a the lab frame which is non-inertial due to the Earth's axial rotation and revolution around the Sun– but the rotation matters most

Consider the approximately inertial Sun Centred Frame (SCF)

The **a** and **c** coefficients would be space-time constants in the SCF but would oscillate in time in the lab frame

$$c_{\text{lab}}^{\mu\nu} = \Lambda^{\mu}{}_{\alpha}\Lambda^{\nu}{}_{\beta}c_{\text{SCF}}^{\alpha\beta}.$$

Thus lab cross sections will oscillate with period controlled by the length of the sidereal day= length of time for the Earth to rotate once wrt the fixed stars ~24hr – 4mins

The SCF

$\hat{Z}$ $T=0$

$\eta \simeq 23.5°$

$\hat{Y}$

$\beta_{\oplus} \simeq 10^{-4}$

$\hat{X}$
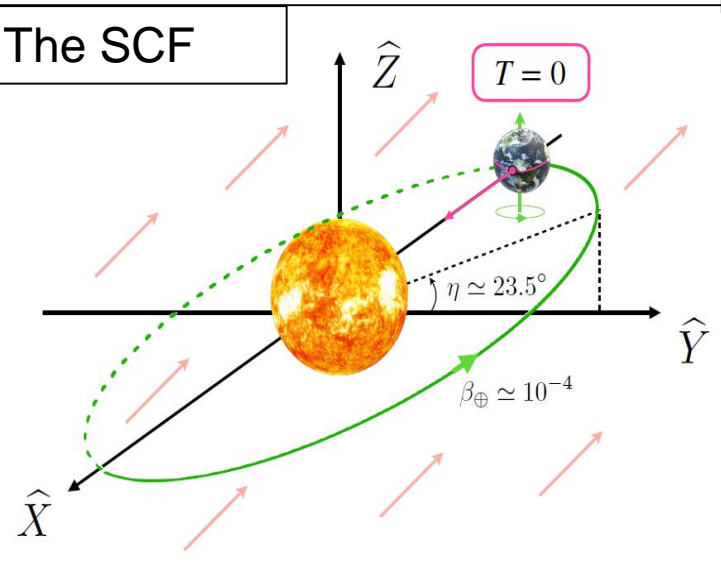
T=0 is the time of the vernal equinox 2000
Z is aligned with the Earth's rotation axis
X points from Earth to Sun at equinox, Y makes rhs
At T=0 the equator is in the XY plane and the longitude λ_0=66.25 will observe the Sun right overhead

We must know the co-latitude of ZEUS, χ = 36.4, the orientation of the beam direction, Ψ = 20 south of west, and the local sidereal time $T_{\oplus}$, the Zero of this is defined when the y axis of the lab is parallel to Y …

HERA is not at longitude λ_0 but at λ = 9.88 and the sidereal day is 23hr 56min 4 sec

So $T_{\oplus} = 0$ is 3.75 hrs after the equinox

$$T - T_{\oplus} = \frac{\lambda_0 - \lambda}{360°}T_{\text{sidereal}} = 3.748 \text{ h},$$

3

So the net rotation from the beam direction in the lab to the SCF is..

$$R = \begin{pmatrix} 1 & 0 & 0 \\ 0 & 0 & 1 \\ 0 & -1 & 0 \end{pmatrix} \begin{pmatrix} \cos\Psi & \sin\Psi & 0 \\ -\sin\Psi & \cos\Psi & 0 \\ 0 & 0 & 1 \end{pmatrix} \begin{pmatrix} \cos\chi\cos\omega_\oplus T_\oplus & \cos\chi\sin\omega_\oplus T_\oplus & -\sin\chi \\ -\sin\omega_\oplus T_\oplus & \cos\omega_\oplus T_\oplus & 0 \\ \sin\chi\cos\omega_\oplus T_\oplus & \sin\chi\sin\omega_\oplus T_\oplus & \cos\chi \end{pmatrix}$$

Where $\omega_\oplus = 2\pi/T_{\text{sidereal}}$ s the sidereal frequency.

Thus the **c** coefficients in the SCF frame c^{XX}, c^{YY} etc will appear in the lab frame as, eg

$$\begin{aligned} c_u^{33} &= \frac{1}{2}(c_u^{XX} + c_u^{YY})\left(\cos^2\chi\sin^2\Psi + \cos^2\Psi\right) + c_u^{ZZ}\sin^2\chi\sin^2\Psi \\ &\quad -2c_u^{XZ}\sin\chi\sin\Psi\left[\cos\chi\sin\Psi\cos(\omega_\oplus T_\oplus) + \cos\Psi\sin(\omega_\oplus T_\oplus)\right] \\ &\quad -2c_u^{YZ}\sin\chi\sin\Psi\left[\cos\chi\sin\psi\sin(\omega_\oplus T_\oplus) - \cos\psi\cos(\omega_\oplus T_\oplus)\right] \\ &\quad +c_u^{XY}\left[(\cos^2\chi\sin^2\Psi - \cos^2\Psi)\sin(2\omega_\oplus T_\oplus) - \cos\chi\sin(2\Psi)\cos(2\omega_\oplus T_\oplus)\right] \qquad (15) \\ &\quad +\frac{1}{2}(c_u^{XX} - c_u^{YY})\left[(\cos^2\chi\sin^2\Psi - \cos^2\Psi)\cos(2\omega_\oplus T_\oplus) + \cos\chi\sin(2\Psi)\sin(2\omega_\oplus T_\oplus)\right] \end{aligned}$$

With time oscillations in multiples of ω_{sidereal} , where only the following 18 combinations actually lead to oscillations $c_f^{TX}, c_f^{XZ}, c_f^{TY}, c_f^{YZ}, c_f^{XY}$ and $(c_f^{XX} - c_f^{YY})$ $f = u, d, \text{and } s.$

Similarly for **a** coefficients 36 combinations lead to oscillations with frequencies up to 3ω, and since s and sbar are the same only 24 of these are non-zero

$(a_{Sf}^{(5)TXX} - a_{Sf}^{(5)TYY})$, $(a_{Sf}^{(5)XXZ} - a_{Sf}^{(5)YYZ})$, $a_{Sf}^{(5)TXY}$, $a_{Sf}^{(5)TXZ}$, $a_{Sf}^{(5)TYZ}$, $a_{Sf}^{(5)XXX}$,

$a_{Sf}^{(5)XXY}$, $a_{Sf}^{(5)XYY}$, $a_{Sf}^{(5)XYZ}$, $a_{Sf}^{(5)XZZ}$, $a_{Sf}^{(5)YYY}$ and $a_{Sf}^{(5)YZZ}$,

Study performed on HERA-II data, 372 pb^{-1} of data at E$_p$= 920GeV and E$_e$=27.5 GeV, $\sqrt{s}$ = 318 GeV, Neutral Current events

- the final-state lepton was identified using an algorithm based on a neural network [31, 32], giving a probability larger than 90%;

- the energy of the final-state lepton $E'_e > 10$ GeV to ensure a high electron-identification efficiency;

- $Q^2 > 5$ GeV^2;

- $\theta_e > 1$ rad, where θ_e is the scattering angle between the outgoing lepton and incoming proton direction to ensure the high efficiency of the electron-identification algorithm.

- the scattered lepton was required to enter the calorimeter at a radial position larger than 15 cm, implying an upper bound on the lepton scattering angle $\theta_e \lesssim 3$ rad;

- the position of the event vertex along the laboratory z axis was required to be within 30 cm of its nominal value and the transverse distance of the event vertex from the interaction point was required to be within 0.5 cm, to reject background;

- 47 GeV $< E - p_z < 69$ GeV, where E and p_z are the total energy and z-component of the final state, to reject background.

This selection resulted in $4.5 \cdot 10^7$ events covering the kinematic range $7.7 \cdot 10^{-5} < x_{\text{Bj}} < 1$ and $5 < Q^2 < 8800$ GeV^2.

We study $\dfrac{d\sigma}{dx_{\text{Bj}}\, dQ^2\, d\phi_{T_{\text{p}}}}$ where $\phi_{T_{\text{p}}} = \text{Mod}(T_\oplus, T_{\text{p}})/T_{\text{p}}$ is the phase of the

event with time stamp $T_\oplus$ for the period T_p defined in the range 0 to 1,

Only the choice of period $T_p = T_{sidereal}$ gives a genuine non-vanishing dependence on the phase.

However, there can be a dependence on instantaneous luminosity
SO what is actually done is to take double ratios of the phase dependence, for two regions of the x, Q^2 plane, PS_1 and PS_2, for which the luminosity uncertainty cancels

$$r(\text{PS}_1, \text{PS}_2) = \frac{\int_{\text{PS}_1} dx_{\text{Bj}} dQ^2 \frac{d\sigma}{dx_{\text{Bj}}\, dQ^2\, d\phi_{T_{\text{p}}}} \Big/ \int_{\text{PS}_1} dx_{\text{Bj}} dQ^2 d\phi_{T_{\text{p}}} \frac{d\sigma}{dx_{\text{Bj}}\, dQ^2\, d\phi_{T_{\text{p}}}}}{\int_{\text{PS}_2} dx_{\text{Bj}} dQ^2 \frac{d\sigma}{dx_{\text{Bj}}\, dQ^2\, d\phi_{T_{\text{p}}}} \Big/ \int_{\text{PS}_2} dx_{\text{Bj}} dQ^2 d\phi_{T_{\text{p}}} \frac{d\sigma}{dx_{\text{Bj}}\, dQ^2\, d\phi_{T_{\text{p}}}}}$$

This ratio will simply be unity if there are no SME LV effects, but choosing the regions of phase space carefully can yield strong deviations from unity if there are such effects
An optimal choice is to look at events above and **below an x cut of $x_c=10^{-3}$ for both c and a coefficients**, since although c coefficients are in principal more sensitive to low x--- involving $d\sigma \propto (f_f + f_{\bar{f}})$ rather than $d\sigma \propto (f_f - f_{\bar{f}})$, ------------

we do not wish to enter the region where QCD BFKL effects complicate the analysis..
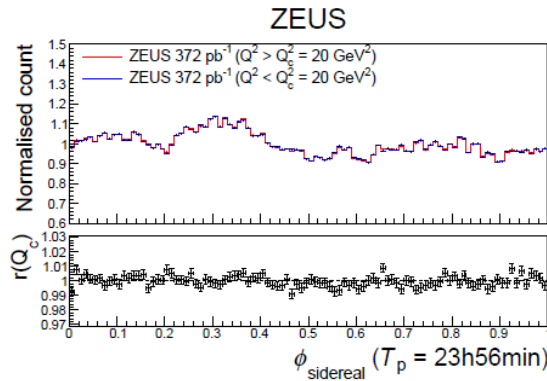
But we must test for systematic effects.
First construct a double ratio that would not be expected to deviate from unity, and check if it does. E.g. consider a Q^2 cut not an x cut, at Q^2_c = 20 GeV².
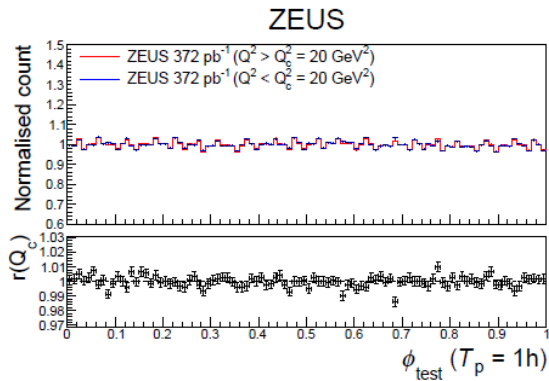
We will check how this ratio behaves when plotted against various time periods
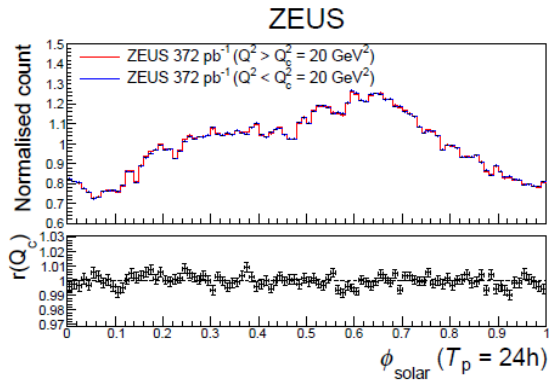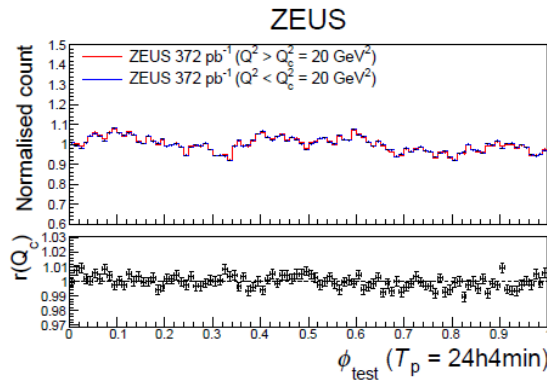

(a)

(b)

(c)

(d)

We expect the variation with the solar day
But it is not washed out for the sidereal day (24hr – 4mins)
Only for very short/long periods is it washed out

We also look at 24hr + 4minutes for calibration

For each choice of phase the histograms taken above and below the cut track each other and their ratio, shown underneath, is close to unity

7

To be sure there are no overall systematic effects we apply Kolmogorov/Smirnov test to these ratios to evaluate what is the probability the distributions are compatible with an unsorted sampling of a normal distribution mean unity and standard deviation compatible with statistical uncertainties.
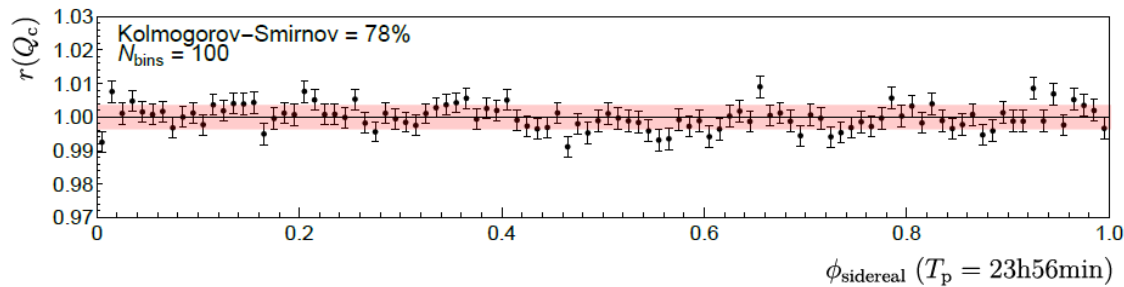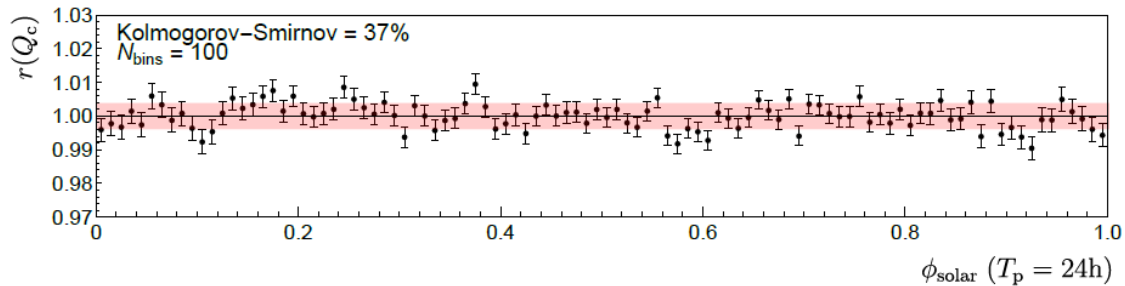
Regardless of the period, solar or sidereal, the ratios using the Q^2 cut are compatible with an assumption of only statistical uncertainties…
This is also true if fewer bins are used to decrease statistical uncertainties

**Now let us look at ratios using the x cut, where we may expect some real Standard Model Extension effects….**

8

For low and high regions of x, the triggers are different and could be affected by the instantaneous luminosity..

For periods such as the solar or sidereal day, the time bins are larger than the duration of one fill so fluctuations in trigger efficiencies and accelerator effects could affect the high and low lumi parts of the fill differently……………
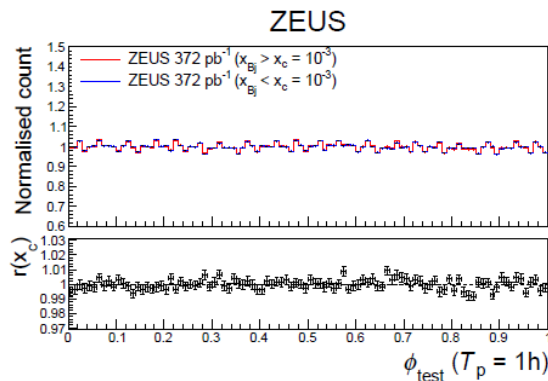
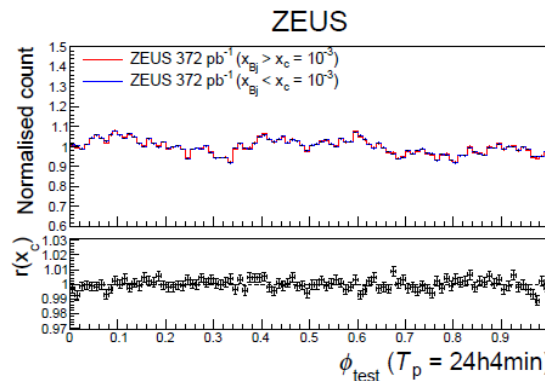so it is not clear that such ratios are systematics free
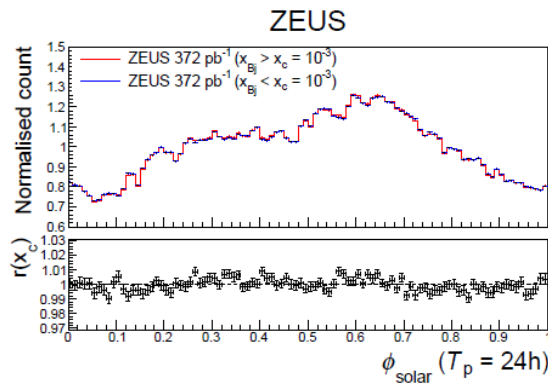
(a)
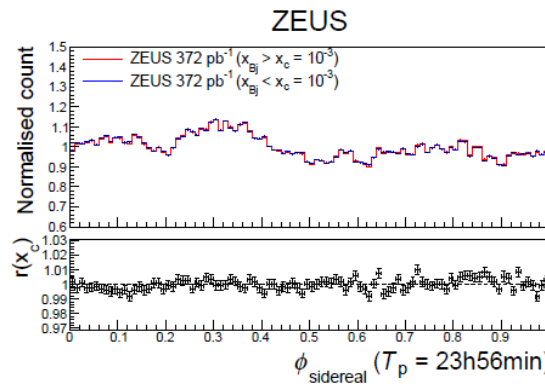
(b)

(c)

(d)

The ratios for the x cut behave very much like those with the Q^2 cut for the different choices of period

But a Kolmogorov-Smirnov test conducted on the solar phase plots shows rather more structure…..

(e.g not so for the phase T=1hr)

9
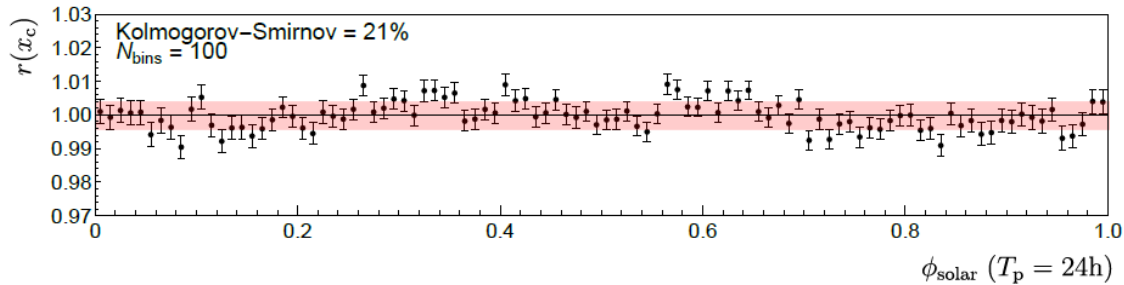
And if the data are binned more coarsely to decrease statistical uncertainties, we can see that the K-S probability is rather low
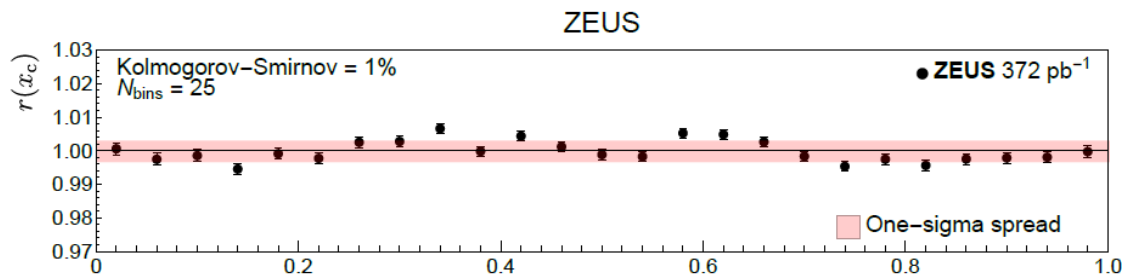
We use can use this to estimate the size of the systematic

$$\sigma_{\text{syst}} \approx \sqrt{\sigma^2 - \sigma_{\text{stat}}^2} \, ,$$

from the spread of this distribution σ and its statistical spread σ_{stat}

10

Such a systematic was not identified before, it is too small to have mattered in previous analyses

We check this out by looking at MC samples of the DIS events (QCD, LO) passed through detector and trigger simulations. Time stamps are applied to the MC samples to simulate time dependence associated with instantaneous luminosity and detector response
BUT there is no evidence of systematic effects in these MC samples…we cannot simulate it, so we just have to estimate it.

The size of the systematic for the solar period is σ_{syst}~0.26%.
We can also calculate it for the periods 24hrs ± 4mins as σ_{syst}~0.16%/0.18% resp.
These smaller values suggest a genuine solar effect that may be a consequence of the operation of the experiment.

Consequently sidereal time effects which we are looking for may be affected by this.
We chose to assign a systematic uncertainty, σ_{syst}~0.16%, from the 24hr+4minutes period as a measure of the dilution of the solar effect when moving by 4mins from 24hr---- independently of the sidereal result.
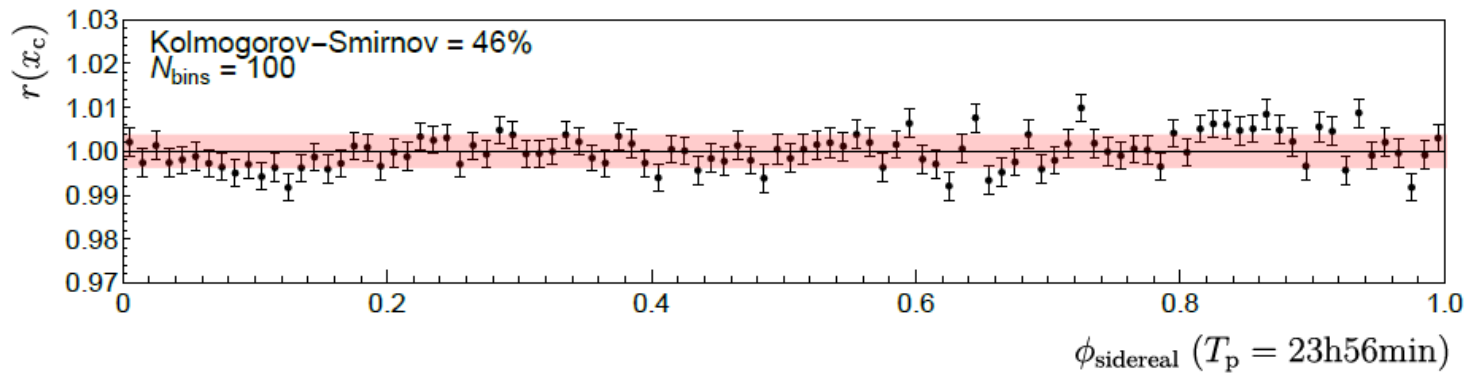
Finally the results are got from the sidereal phase plot for the xcut, $x_c = 10^{-3}$

The theory to be compared to this plot in the SCF is got from the equations

$$
\begin{aligned}
r_c(x_{Bj} > x_c, x_{Bj} < x_c) &= 1 - 12.8\, c_u^{03} - 13.9\, c_u^{33} + 0.9\,(c_u^{11} + c_u^{22}) \\
&\quad - 4.2\, c_d^{03} - 2.9\, c_d^{33} + 0.1\,(c_d^{11} + c_d^{22}) \\
&\quad - 3.4\, c_s^{03} - 1.8\, c_s^{33} + 2.9 \cdot 10^{-2}\,(c_s^{11} + c_s^{22}), \qquad (20)
\end{aligned}
$$

$$
\begin{aligned}
r_{a(5)}(x_{Bj} > x_c, x_{Bj} < x_c) &= 1 - 6.1 \cdot 10^3\, a_u^{(5)003} + 6.8 \cdot 10^3\, a_u^{(5)033} - 2.5 \cdot 10^3\, a_u^{(5)333} \\
&\quad + 5.0 \cdot 10^2\,(a_u^{(5)113} + a_u^{(5)223} - a_u^{(5)011} - a_u^{(5)022}) \\
&\quad - 4.1 \cdot 10^2\, a_d^{(5)003} + 4.7 \cdot 10^2\, a_d^{(5)033} - 1.7 \cdot 10^2\, a_d^{(5)333} \\
&\quad + 40\,(a_d^{(5)113} + a_d^{(5)223} - a_d^{(5)011} - a_d^{(5)022}), \qquad (21)
\end{aligned}
$$

We consider only ONE coefficient at a time and go from the SCF to the lab predictions

.

12

The ratios then depend on the local sidereal angle $\theta_\oplus = \omega_\oplus T_\oplus$.
For each bin

$$r_i^{\text{theo}} = \frac{N_{\text{bins}}}{2\pi} \int_{\frac{2\pi(i-1)}{N_{\text{bins}}}}^{\frac{2\pi i}{N_{\text{bins}}}} r(x > x_c, x < x_c; \theta_\oplus) d\theta_\oplus \ ,$$

This is compared to the data ratio $\quad \chi^2 = \frac{1}{\sigma_{\text{tot}}^2} \sum_{i=1}^{N_{\text{bins}}} \left(r_i^{\text{exp}} - r_i^{\text{theo}}\right)^2$ for each coefficient

where the total uncertainty
includes the statistical ~0.32% and systematic ~0.16% components.

There are 42 SCF coefficients which could make these ratios deviate from unity

The χ2 for the Standard Model—all coefficients zero-- is 113.8 for 100 points, p_{value}=0.16. So the Standard Model is compatible with the data

For each coefficient we present a range of acceptable values with p>0.05
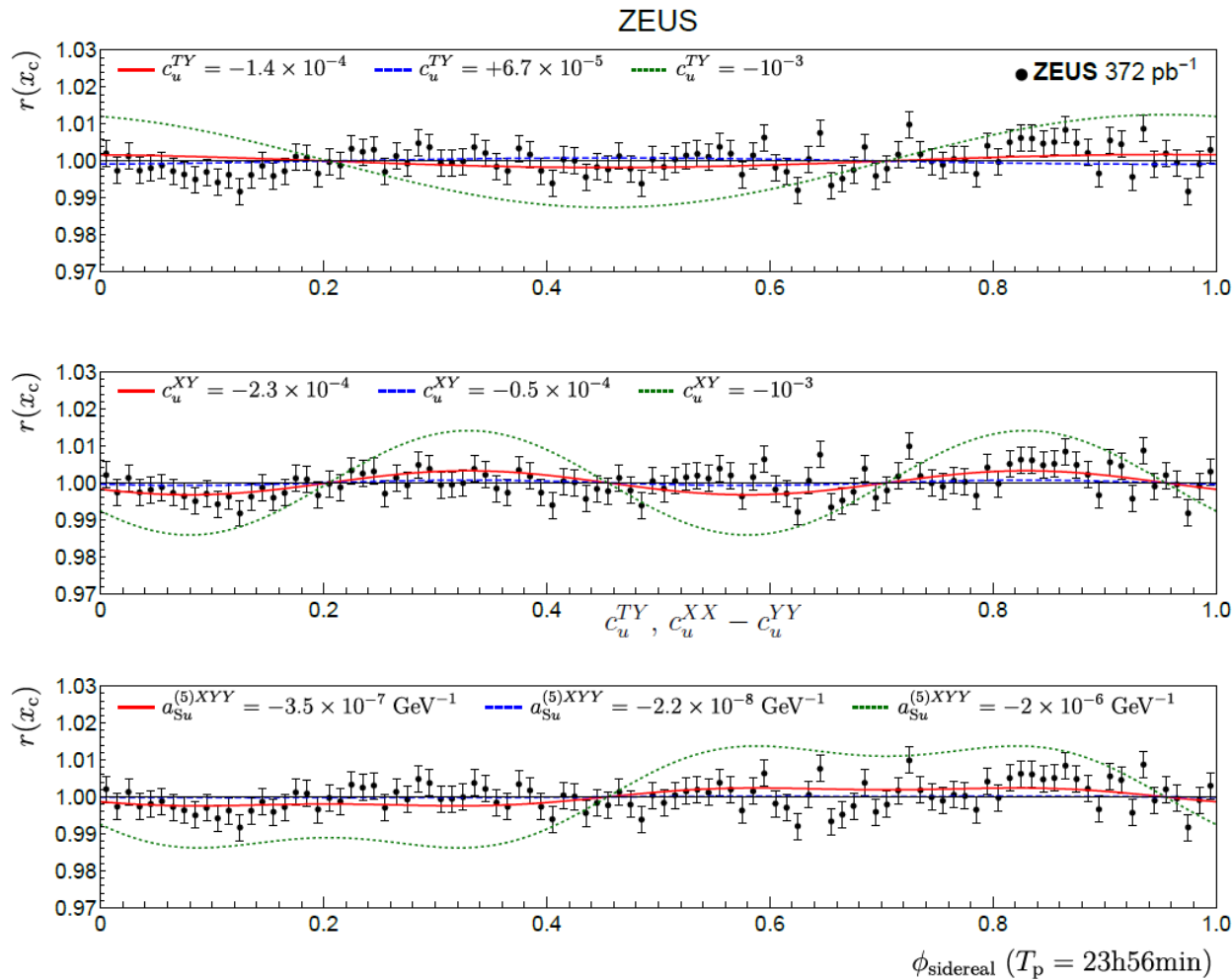
The data is in black the red and blue curves show lower and upper limits from the present analysis, the green curve shows values 10* higher for comparison

The coefficients shown for illustration c_u^{TY}, $c_u^{XX} - c_u^{YY}$ and $a_{Su}^{(5)XXY}$ have periods of $\omega_{\oplus}$, $2\omega_{\oplus}$ and $3\omega_{\oplus}$, respectively.

14

Coefficient	Lower	Upper
c_u^{TX}	-2.5×10^{-4}	6.6×10^{-5}
c_u^{TY}	-1.7×10^{-4}	9.8×10^{-5}
c_u^{XY}	-3.2×10^{-4}	4.1×10^{-5}
c_u^{XZ}	-5.4×10^{-4}	1.4×10^{-4}
c_u^{YZ}	-3.7×10^{-4}	2.1×10^{-4}
$c_u^{XX} - c_u^{YY}$	-2.1×10^{-4}	2.5×10^{-4}
c_d^{TX}	-7.8×10^{-4}	2.0×10^{-4}
c_d^{TY}	-5.2×10^{-4}	3.0×10^{-4}
c_d^{XY}	-1.6×10^{-3}	2.0×10^{-4}
c_d^{XZ}	-2.7×10^{-3}	7.0×10^{-4}
c_d^{YZ}	-1.8×10^{-3}	1.0×10^{-3}
$c_d^{XX} - c_d^{YY}$	-1.0×10^{-3}	1.2×10^{-3}
c_s^{TX}	-9.6×10^{-4}	2.5×10^{-4}
c_s^{TY}	-6.4×10^{-4}	3.7×10^{-4}
c_s^{XY}	-2.6×10^{-3}	3.3×10^{-4}
c_s^{XZ}	-4.4×10^{-3}	1.2×10^{-3}
c_s^{YZ}	-3.0×10^{-3}	1.7×10^{-3}
$c_s^{XX} - c_s^{YY}$	-1.7×10^{-3}	2.0×10^{-3}

Coefficient	Lower (GeV^{-1})	Upper (GeV^{-1})
$a_{Su}^{(5)TXX} - a_{Su}^{(5)TYY}$	-5.1×10^{-7}	4.3×10^{-7}
$a_{Su}^{(5)XXZ} - a_{Su}^{(5)YYZ}$	-1.7×10^{-6}	2.0×10^{-6}
$a_{Su}^{(5)TXY}$	-8.3×10^{-8}	6.5×10^{-7}
$a_{Su}^{(5)TXZ}$	-2.9×10^{-7}	1.1×10^{-6}
$a_{Su}^{(5)TYZ}$	-4.3×10^{-7}	7.4×10^{-7}
$a_{Su}^{(5)XXX}$	-3.9×10^{-7}	1.2×10^{-7}
$a_{Su}^{(5)XXY}$	-2.3×10^{-7}	1.8×10^{-7}
$a_{Su}^{(5)XYY}$	-4.6×10^{-7}	9.2×10^{-8}
$a_{Su}^{(5)XYZ}$	-2.6×10^{-6}	3.3×10^{-7}
$a_{Su}^{(5)XZZ}$	-5.4×10^{-7}	1.4×10^{-7}
$a_{Su}^{(5)YYY}$	-2.9×10^{-7}	1.5×10^{-7}
$a_{Su}^{(5)YZZ}$	-3.6×10^{-7}	2.1×10^{-7}
$a_{Sd}^{(5)TXX} - a_{Sd}^{(5)TYY}$	-7.3×10^{-6}	6.1×10^{-6}
$a_{Sd}^{(5)XXZ} - a_{Sd}^{(5)YYZ}$	-2.4×10^{-5}	2.8×10^{-5}
$a_{Sd}^{(5)TXY}$	-1.2×10^{-6}	9.4×10^{-6}
$a_{Sd}^{(5)TXZ}$	-4.1×10^{-6}	1.6×10^{-5}
$a_{Sd}^{(5)TYZ}$	-6.1×10^{-6}	1.1×10^{-5}
$a_{Sd}^{(5)XXX}$	-5.7×10^{-6}	1.7×10^{-6}
$a_{Sd}^{(5)XXY}$	-3.4×10^{-6}	2.7×10^{-6}
$a_{Sd}^{(5)XYY}$	-6.8×10^{-6}	1.3×10^{-6}
$a_{Sd}^{(5)XYZ}$	-3.7×10^{-5}	4.6×10^{-6}
$a_{Sd}^{(5)XZZ}$	-8.1×10^{-6}	2.1×10^{-6}
$a_{Sd}^{(5)YYY}$	-4.3×10^{-6}	2.3×10^{-6}
$a_{Sd}^{(5)YZZ}$	-5.4×10^{-6}	3.1×10^{-6}

For the **c** coefficients these are the first limits from sidereal oscillations
Constraints on the u, d exist from cosmic rays but are model dependent
The s constraints are the first ever.

The constraints on the **a** coefficients are all the first ever

One can also estimate sensitivities for the EIC

	HERA	EIC
$\left\| a_{Su}^{(5)TXX} - a_{Su}^{(5)TYY} \right\|$	7.0×10^{-6}	2.3×10^{-6}
$\left\| a_{Su}^{(5)XXZ} - a_{Su}^{(5)YYZ} \right\|$	1.8×10^{-5}	5.2×10^{-6}
$\left\| a_{Su}^{(5)TXY} \right\|$	2.3×10^{-6}	3.4×10^{-7}
$\left\| a_{Su}^{(5)TXZ} \right\|$	4.7×10^{-6}	1.3×10^{-7}
$\left\| a_{Su}^{(5)TYZ} \right\|$	4.6×10^{-6}	1.3×10^{-7}
$\left\| a_{Su}^{(5)XXX} \right\|$	1.7×10^{-6}	1.4×10^{-7}
$\left\| a_{Su}^{(5)XXY} \right\|$	1.6×10^{-6}	1.4×10^{-7}
$\left\| a_{Su}^{(5)XYY} \right\|$	1.6×10^{-6}	1.4×10^{-7}
$\left\| a_{Su}^{(5)XYZ} \right\|$	1.0×10^{-5}	4.3×10^{-7}
$\left\| a_{Su}^{(5)XZZ} \right\|$	2.1×10^{-6}	1.2×10^{-7}
$\left\| a_{Su}^{(5)YYY} \right\|$	1.7×10^{-6}	1.4×10^{-7}
$\left\| a_{Su}^{(5)YZZ} \right\|$	2.1×10^{-6}	1.2×10^{-7}

EIC improvements over HERA are due to much larger expected luminosity

Summary

Standard Model Extensions with Lorentz Violation using 4D and 5D operators in context of Effective Field Theory would induce sidereal time dependence on DIS cross sections

ZEUS data has been used to study this.
Systematic effects due to variations of instantaneous luminosity are carefully eliminated/estimated

The Standard Model describes that data with p value 0.16

Upper and lower limits are set on the vector and tensor coefficients of the Standard Model Extension in the quark sector. Many of these are constrained for the first time.

$$\frac{d\sigma}{dx_{\text{Bj}}dy_{\text{Bj}}d\varphi} = \frac{\alpha^2 y_{\text{Bj}}}{2Q^4} \sum_f e_f^2 \frac{1}{\widetilde{Q}_f^2} L_{\mu\nu} H_f^{\mu\nu} f_f(\widetilde{x}_f) \,,$$

where φ is the scattered lepton azimuthal angle, $\widetilde{Q}_f^2 = -\widetilde{q}_f^2 = -(q^\mu + c_f^{\mu q})(q_\mu + c_{f\mu q})$ where $c_f^{\mu q} \equiv c_f^{\mu\nu} q_\nu$,

$$
\begin{aligned}
L_{\mu\nu} H_f^{\mu\nu} = {} & 8 \Big[2(\widehat{k}_f \cdot l)(\widehat{k}_f \cdot l') + \widehat{k}_f \cdot (l - l')(l \cdot l') + 2(\widehat{k}_f \cdot l) \left(c_f^{\widehat{k}_f l'} + c_f^{l'\widehat{k}_f} - c_f^{l'l'} \right) \\
& + 2(\widehat{k}_f \cdot l') \left(c_f^{\widehat{k}_f l} + c_f^{l\widehat{k}_f} + c_f^{ll} \right) - 2(l \cdot l') c_f^{\widehat{k}_f \widehat{k}_f} \Big] \,,
\end{aligned}
$$

with $\widehat{k}_f^\mu = \widetilde{x}_f(p^\mu - c_f^{\mu p})$. The parton distribution functions (PDFs) are denoted $f_f(\widetilde{x}_f)$ and are evaluated at the shifted Bjorken variable [9]

$$\widetilde{x}_f = x_{\text{Bj}} \left(1 + \frac{2c_f^{qq}}{q^2} \right) + \frac{x_{\text{Bj}}^2}{q^2} \left(c_f^{pq} + c_f^{qp} \right) , \tag{7}$$

where $c_f^{qq} \equiv c_f^{\mu\nu} q_\mu q_\nu$, etc. '

19

The cross section including effects of the $a^{(5)}$-type coefficients from Eq. (3) is [6,9]

$$
\frac{d\sigma}{dx_{\mathrm{Bj}}dy_{\mathrm{Bj}}d\varphi} = \frac{\alpha^2}{Q^4}\sum_f F_{2f}\left[\frac{y_{\mathrm{Bj}}s^2}{\pi}\left[1+(1-y_{\mathrm{Bj}})^2\right]\delta_{\mathrm{S}f}+\frac{y_{\mathrm{Bj}}(y_{\mathrm{Bj}}-2)s}{x_{\mathrm{Bj}}}x_{\mathrm{S}f}\right.
$$

$$
-\frac{4}{x_{\mathrm{Bj}}}\left(4x_{\mathrm{Bj}}^2 a_{\mathrm{S}f}^{(5)ppl}+6x_{\mathrm{Bj}}a_{\mathrm{S}f}^{(5)lpq}+2a_{\mathrm{S}f}^{(5)lqq}\right)
$$

$$
+2y_{\mathrm{Bj}}\left(4x_{\mathrm{Bj}}^2 a_{\mathrm{S}f}^{(5)ppp}+4x_{\mathrm{Bj}}a_{\mathrm{S}f}^{(5)ppq}+4x_{\mathrm{Bj}}a_{\mathrm{S}f}^{(5)lpp}+2a_{\mathrm{S}f}^{(5)lpq}+a_{\mathrm{S}f}^{(5)pqq}\right)
$$

$$
\left.+\frac{4y_{\mathrm{Bj}}}{x_{\mathrm{Bj}}}\left(2x_{\mathrm{Bj}}a_{\mathrm{S}f}^{(5)llp}+a_{\mathrm{S}f}^{(5)llq}\right)\right], \tag{8}
$$

where $F_{2f}=e_f^2 f_f(x'_{\mathrm{S}f})x'_{\mathrm{S}f}$ with $x'_{\mathrm{S}f}=x_{\mathrm{Bj}}-x_{\mathrm{S}f}$ and

$$
\delta_{\mathrm{S}f} = \frac{\pi}{y_{\mathrm{Bj}}s}\left[1+\frac{2}{y_{\mathrm{Bj}}s}\left(4x_{\mathrm{Bj}}a_{\mathrm{S}f}^{(5)ppq}+3a_{\mathrm{S}f}^{(5)pqq}\right)\right], \tag{9}
$$

$$
x_{\mathrm{S}f} = -\frac{2}{y_{\mathrm{Bj}}s}\left(2x_{\mathrm{Bj}}^2 a_{\mathrm{S}f}^{(5)ppq}+3x_{\mathrm{Bj}}a_{\mathrm{S}f}^{(5)pqq}+a_{\mathrm{S}f}^{(5)qqq}\right), \tag{10}
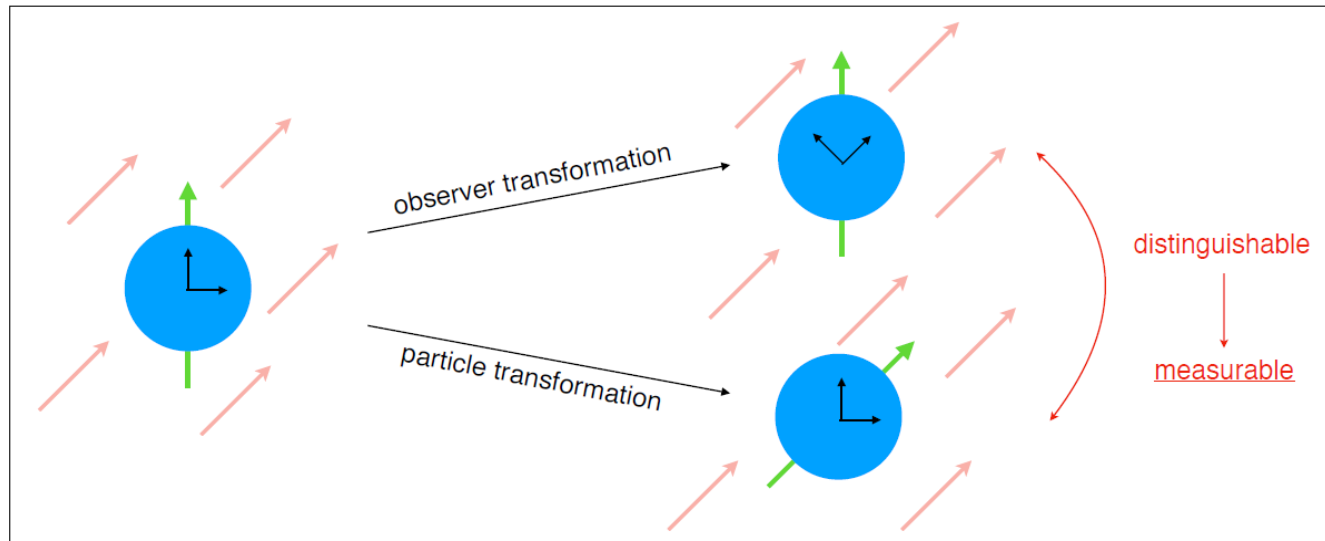$$

$$
a_{\mathrm{S}f}^{(5)\mu\alpha\beta} = \frac{1}{3}\sum_{(\mu\alpha\beta)}\left(a_f^{(5)\mu\alpha\beta}-\frac{1}{6}a_f^{(5)\mu\rho\sigma}\eta_{\rho\sigma}\eta^{\alpha\beta}-\frac{1}{3}a_f^{(5)\rho\mu\sigma}\eta_{\rho\sigma}\eta^{\alpha\beta}\right), \tag{11}
$$

where $a_{\mathrm{S}f}^{(5)qqq}\equiv a_{\mathrm{S}f}^{(5)\mu\alpha\beta}q_\mu q_\alpha q_\beta$, etc. The sum in Eq. (11) denotes symmetrisation with

- A rotation of the observer cannot be distinguished from an opposite rotation of the system

observer transformation

particle transformation

indistinguishable
from observer
point of view
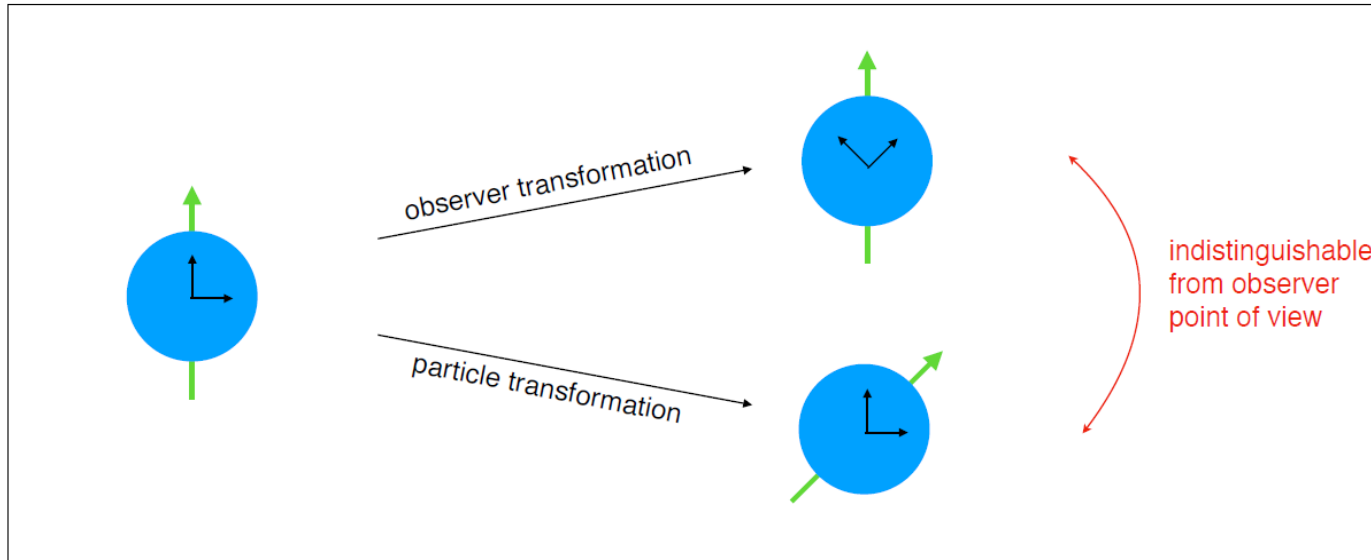
- In presence of a directional background, the two rotations are inequivalent

observer transformation

particle transformation

distinguishable

measurable

= observer (reference frame)   = particle (actual physical system)   = Lorentz-violating background field

2) Some situations can be described in terms of an effective or apparent Lorentz violation (e.g. dark matter wind)

dark-matter halo

galactic disk

Sun-Earth system

DM wind

$v \simeq 10^{-3}c$
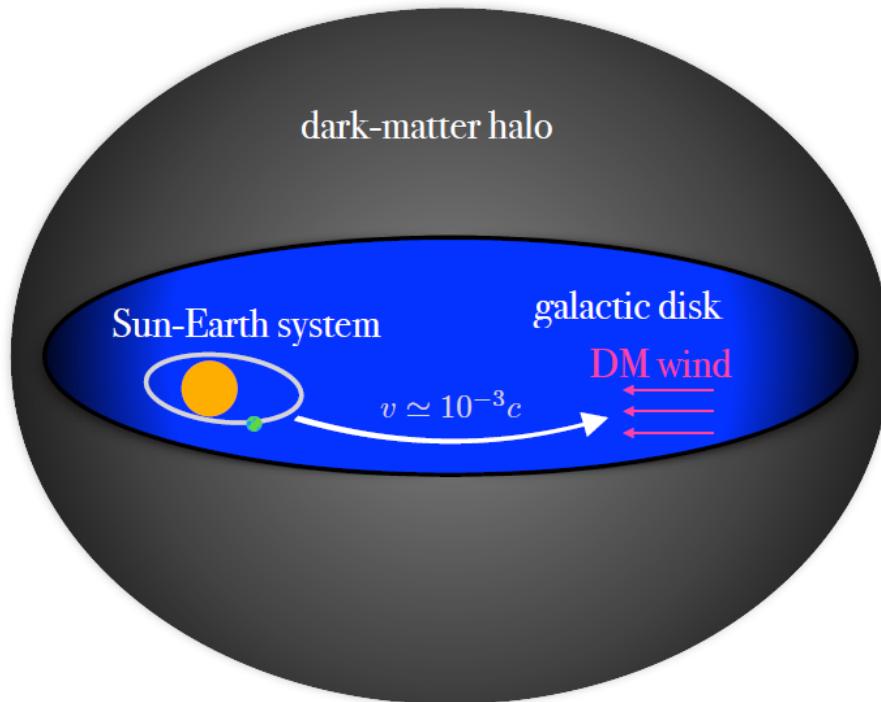
- In Sun-Earth system frame, a velocity-dependent dark matter "wind" is observed

- Produces daily variations ("rotation violation")

- Produces annual variations ("boost violation")

- In this example, dark matter interactions are Lorentz invariant, but lead to apparent Lorentz violation!

Sensitivities to such coefficients across the x,y Q² plane
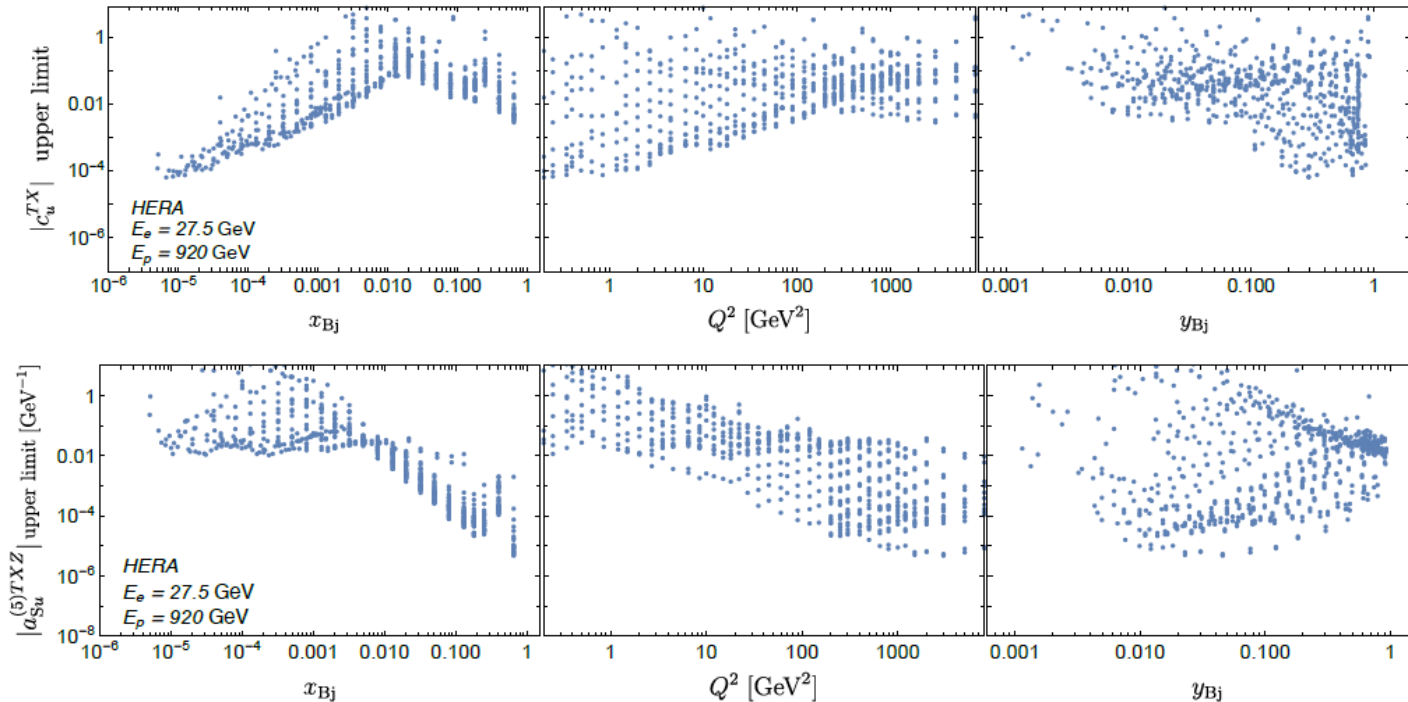
Figure 3: *Regions in x_{Bj}, Q^2 and y_{Bj} that have sensitivity to Lorentz-violating effects for a single c-type and $a^{(5)}$-type coefficient. The points displayed in the plots are taken from Figures 2 and 4 of Ref. [9], where no experimental restrictions on the kinematic region have been considered.*